

Type of the Paper: Proceedings

Aurone as promising human pancreatic lipase inhibitors through *in silico* study

Han Ai Huynh, Dat Van Truong, Van Thi Cam Vo, Phuong Thuy Viet Nguyen* and Dao Thanh Tran*

Affiliation: Faculty of Medicine and Pharmacy at Hochiminh city, Viet Nam

* Correspondence: Phuong Thuy Viet Nguyen – email: ntvphuong@ump.edu.vn - Tel.: +084-919520708; Dao Thanh Tran – email: tranthanhdao@uphcm.edu.vn - Tel.: +084-903716482.

† Presented at the title, place, and date.

Received: date; Accepted: date; Published: date

Abstract: In this study, 82 aurone compounds, a subclass of flavonoids were investigated towards to human pancreatic lipase inhibitory activity. Molecular docking of the aurones was done successfully into the catalytic position of lipase (Pdb: 1LPB) using AutoDock Vina software 1.5.7.rc1. The results showed that 62 compounds interacted well with residues in the catalytic triad Ser152-Asp176-His263 and Phe77 of protein 1LPB. In particular, A32 was selected as the best binding compound (docking score: $-10.6 \text{ kcal.mol}^{-1}$) and suitable for oral drug following the 5-Lipinski rule. Combining the results of docking and molecular dynamics simulation of A32- protein complex during 10 ns, this study performed that the A32 compound bound well and formed a stable complex with 1LPB protein. Therefore, the A32 compound was considered as the lead compound which could be synthesized and tested for pancreatic lipase inhibitor.

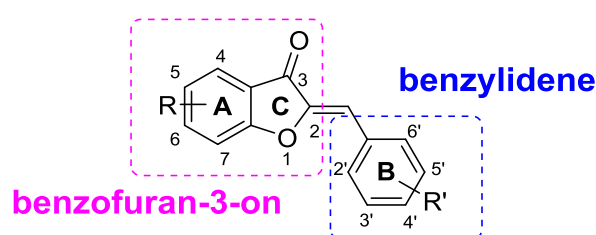
Keywords: aurone, human pancreatic lipase, *in silico*, molecular docking, molecular dynamics simulation.

1. Introduction

Obesity is considered as a complex disease, with a variety of factors and causes, in which the most commonly is an unreasonable diet and unhealthy lifestyle leading to an imbalance between energy supplement and energy consumption in the body [1]. It opens up the way for for the obesity drug research, which is the inhibition of fat hydrolysis of human pancreatic lipase (HPL). Cause, HPL along with co-factors Colipase and Ca^{2+} , play a main role in the process digestion and absorption of fat. HPL hydrolyzes 50 - 70% of the total fat from the food, so inhibiting HPL will significantly reduce the amount of absorbed fat [2, 3].

Nowadays, many *in silico* models are being applied to finding potential bioactive compounds for the treatment of obesity [2, 4, 5-7]. These models made the new drug research more clearly oriented and helped to save both cost and time. Besides that, there is a need to develop new drugs having fewer side effects and more safety, specifically taking from natural compounds for HPL inhibitory activities. The results have discovered natural compounds belonging to many different groups of structures such as saponins, alkaloids, carotenoids, flavonoids that inhibited HPL enzyme [2, 4]. In particular, flavonoids with subclasses such as flavone, flavonole, chalcone have been extensively studied and the researches obtained many good HPL inhibition results with the IC_{50} values determined as Licochalcone A (IC_{50} 35 $\mu\text{g/ml}$) [5], Galangin (IC_{50} 48.20 mg/ml) [6], Hesperidin (IC_{50} 32 $\mu\text{g/ml}$) [7], etc.

Aurone (Figure 1) (IUPAC name is 2-benzylidene-1-benzofuran-3(2H)-on) is a potential subclass of flavonoid. Aurone plays an important role in the pigmentation of some type of flowers and fruits, which is typically bright yellow. They are also found in bark, wood, and leaves. Aurone is considered being phytoalexin, which is used by plants as a defense mechanism against infections. Aurone is often found in some species of the Scrophulariaceae and Compositae families [8, 9]. Many of the biological effects of aurone derivatives have been studied and published as anticancer, anti-inflammatory, antifungal, antibacterial, anti-malarial, anti-hepatitis B, anti-oxidant, etc [10]. However, the inhibition HPL ability of aurone compounds has not been studied, therefore this study conducted molecular docking of aurone derivatives to human pancreatic lipase protein (PDB ID: 1LPB) and investigated the molecular dynamics simulation of the best binding derivative, that contributes to expanding on the HPL potential inhibition of aurone compounds.



R, R': OH, OMe, CH₃, halogen, etc

Figure 1. Structure of aurone frame

2. Materials and methods

2.1. Protein

The 3D structure of the lipase-colipase complex has a crystallized ligand in the catalytic cavity (PDB ID: 1LPB) which was retrieved from Protein Data Bank (<https://www.rcsb.org>). The lipase chain has 449 amino acids, including N-terminal from amino acids 1 to 335 and C-terminal from amino acids 336 to 449, which were attached to colipase. The protein is a crystalline structure with its ligand methoxy undecyl phosphonic acid (MUP). MUP binds and creates bonds with the catalytic cavity of HPL including the hydrogen bonds (H-bonds) with Phe77, Leu153, His263 and the covalent bonds with Ser152 [3, 11-14].

From the retrieved protein structure, protein chains binding with co-crystallization ligands were identified and extracted, and also added polarized hydrogens by AutoDock Tools 1.5.7rc1.

2.2. Ligand

The test compounds consisted of 82 aurone derivatives (symbols A1 to A82) collected from scientific papers investigating the biological effects of aurone derivatives [10, 15-20]. The 2D structures of these compounds were drawn by ISIS Draw 2.5 program and formatted in the MOL file. All 2D structures were converted to 3D structures and they were minimized energies with the YASARA Energy Minimization server (<https://www.yasara.org>).

2.3. Molecular docking

Molecular docking is a method to predict the structure and spatial orientation of one molecule when attached to another molecule to make the most stable complex. There are three common types of

docking: rigid docking, flexible docking, and full flexible docking. A process that simulates ligand and protein binding will involve two basic steps: sampling and scoring [21, 22].

The molecular docking process was implemented by AutoDock Vina software version 1.1.2 [21]. The binding site parameters (x: 8,431; y: 24,417; z: 52,623) and the docking box dimensions (18x18x18 Å) were determined through the re-docking of co-crystallization ligand in the catalytic cavity. The results of molecular docking were evaluated through the criteria of binding structure, binding energy, possible interactions between ligand and residues of the protein.

2.4. Five-lipinski rule

The five-Lipinski rule evaluates a chemical compound, which has a defined chemical and physical property, capable of being researched into an oral drug when it violates no more than one of the following criteria:

- No more than 5 H-bond donors (the sum of NHs and OHs)
- No more than 10 H-bond acceptors (the sum of Ns and Os)
- Log P is less than 5
- MWT less than 500 Da [23]

2.5. Molecular dynamics simulation (MDs)

MDs investigates durability and motion of components (atoms, molecules, particles, etc.) under the influence of environments such as temperature, pressure, and solvent. MDs have performed on the theoretical basis that Newton's second law describes the classical motion of atoms:

$$\vec{F}_i = m_i \vec{a}_i \quad (1)$$

(where \vec{F}_i is force on the atom, m_i is mass of the atom, and a_i is the atom's accelerator) [24].

GROMACS 2018.01 software was used for the MDs of protein without ligand (apoprotein) and protein-ligand complex. From the result of docking, choosing the best configuration of the best binding compound and then adding hydrogen to it by Avogadro ver 1.2.0n software were done. The topology of the ligand structure was created by CGENFF with force field CHARMM36. The test system was put in a simulation box and placed it 1.0 nm from the box edge, which was a 12 surface polyhedron and contained the water solvent of the TIP3P model. Na⁺, Cl⁻ ions were added to the system to balance the charge. The process of energy minimization took place to eliminate the negative interactions in the system. The system was balanced under the "isothermal-isobaric" conditions NVT (N: number of particles, V: volume and T: temperature 300K) and NPT (N: number of particles, P: pressure 1 bar and T: temperature 300K). Berendsen thermostat and Parrinello-Rahman barostat were used to maintain the temperature and pressure. This equilibrium process lasted 1000 ps for each NVT and NPT system. The system were run MDs for 10 ns, at a temperature of 300 °K, and pressure of 1 bar.

The result was recorded every 0.01 ns and evaluated through RMSD (Root-mean-square deviation), RMSF (Root-mean-square fluctuation), Rg (Radius of gyration) and SASA (Solvent-accessible surface area). The parameters were calculated by software GROMACS, VMD version 1.9.3 [25] and were represented as a chart by Microsoft Excel 2016.

3. Results and discussion

3.1. Molecular docking

The 82 aurone derivatives were successfully bond to the catalytic cavity with the docking score ranging from $-10.6 \text{ kcal.mol}^{-1}$ to $-7.4 \text{ kcal.mol}^{-1}$. Of these, 62 compounds were classified into group A. Group A created hydrogen bond with residues in the catalyst trial Ser152-Asp176-His263 and Phe77, which played an important role in the fat hydrolysis activity of pancreatic lipase enzyme. The remaining 20 compounds did not interact with the important residues, which were classified into group B.

62 compounds of group A were classified into 7 subgroups according to their similar structure and position (Table 1, 2).

Table 1. Subgroups 1A, 2A, 3A of group A in aurone compounds

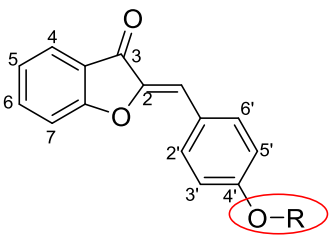
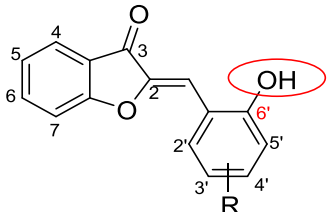
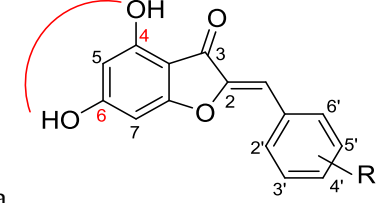
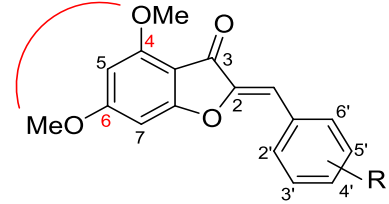
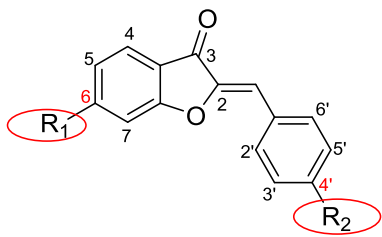
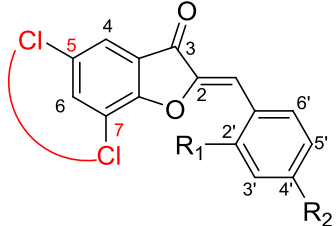
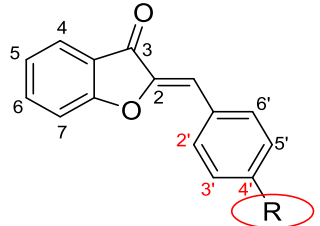
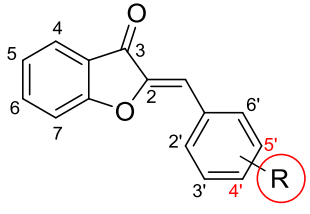
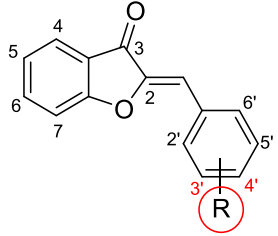
Subgroup	Structure frame of subgroup	Substituents	Compound
1A		R: The aromatic ring with multi-function group	3 compounds: A32, A74, A75
2A		R: CH ₃ , OMe, halogen	3 compounds: A1, A5, A6
3A			7 compounds: A12, A14-15, A26, A33, A42, A81
3A-b		R: alkyl, OH, OMe	12 compounds: A9-11, A31, A34, A36-40, A46, A78

Table 2. Subgroup 4A, 5A, 6A, 7A of group A in aurone compounds

Subgroup	Structure frame of subgroup	Substituents	Compound
4A		R1: OH, OMe, alkyl oxy R2: OH, OMe, halogen, CF3	11 compounds: A20, A29, A30, A41, A43, A44, A50, A52-55
5A		R1: OMe, Br, Cl or R2: CH3, Br, Cl	6 compounds: A60-62, A57-59
6A		R: CH3, OH, OMe, halogen (Br, F, Cl)	9 compounds: A3-4, A8, A48-49, A63, A77, A80, A82.
7A	7A-a 		7 compounds: A18, A19, A25, A47, A51, A56, A73
	7A-b 	R: OH, OMe	3 compounds: A13, A21, A79

In general, there are some comments for the compounds of group A:

- 6'-hydroxy-aurone derivatives (subgroup 2A) and 4,6-dihydroxy-aurone (subgroup 3A-a) were more able to interact with the catalytic cavity than other derivatives. Because the hydroxyl substituent (OH) polarized and stayed in a favorable position for creating hydrogen bonding. In the same position, the methoxy substituent (OMe) gained the results not as good as the results of the OH substituents.
- The aromatic ring with multi-function group substituents in position 4 of the benzylidene ring (subgroup 1A) both increased the ability to create bonds and increased the length of the structure but did not hinder the compound binding to the catalytic cavity.
- The compounds had the small substituents (OH, CH₃, OMe, halogen) in the benzylidene ring (subgroup 6A), whose the results of docking were not much different than the results of docking aurone frame.

Subgroup 1A (Table 1): The docking scores were the best. Especially, compound A32 with a docking score of $-10.6 \text{ kcal.mol}^{-1}$ was the lowest in the subgroup 1A and the lowest among all test compounds. The substituent at 4' of the benzylidene ring increased the length of the structure, pushing the aurone's benzofuran frame to slide out of the catalytic cavity, away from the main residues, so the hydrogen bonds with residues Ser152 and His263 were created by oxygen ether at the 4' position of the benzylidene ring (Figure 2).

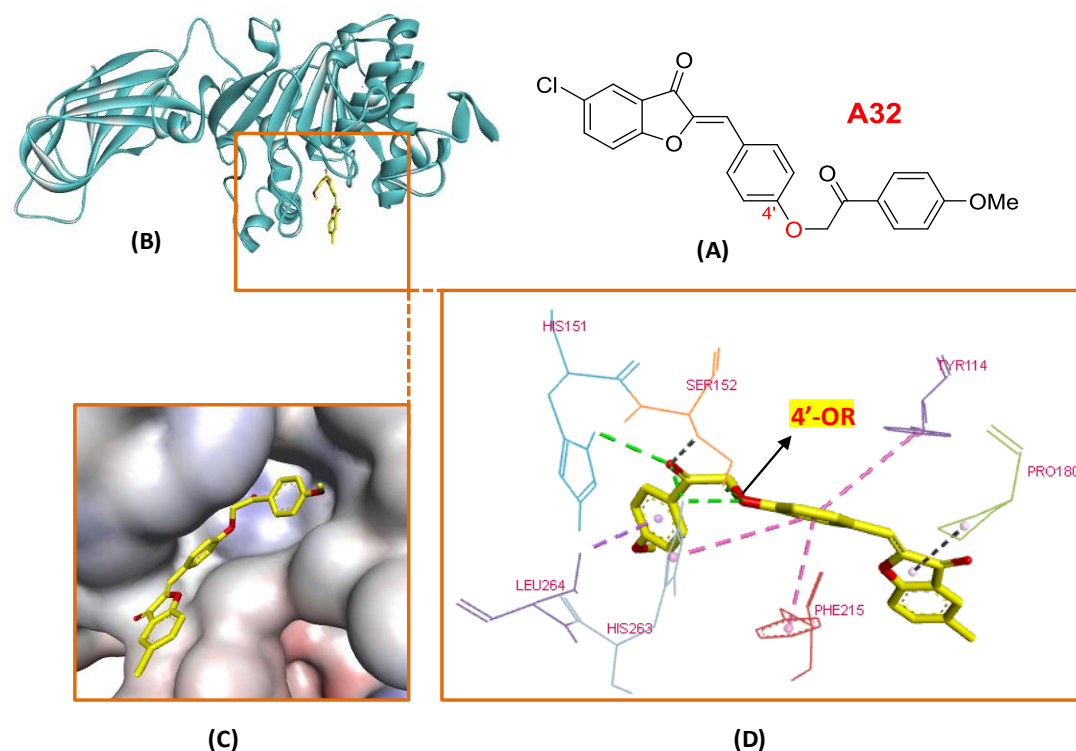


Figure 2. The docking results of compound A32 with protein (PDB ID: 1LPB). (A) 2D structure of the A32 compound. (B) A32 in the catalytic cavity of ribbon protein. (C) A32 in the catalytic cavity of the protein. (D) Interactions of A32 with the catalytic cavity: green is hydrogen bonding, purple is hydrophobic interaction.

Subgroup 2A (Table 1): The docking scores of subgroup 2A were nearly as good as subgroup 1A. The OH substituent at position 6' of the benzylidene ring created an additional hydrogen bond with Ser152.

Subgroup 3A (Table 1): Subgroup 3A-a had an additional OH substituent at position 4, which could make hydrogen bonds with important residues such as Ser152, Phe77, His263 to increase the interaction with the catalyst cavity. Therefore, the compounds with OH substituent at position 4,6 had better docking scores than those with OMe substituents.

The substituents and their positions of subgroups 4A, 5A, 6A, and 7A (Table 2) did not change the structure of the aurone frame much. Therefore, the compounds of these groups inside the catalytic cavity and their bonds with important residues (Ser152- Asp176- His 263 and Phe77) were made up of the aurone frame.

Subgroup B: Subgroup B consisted of 20 compounds, which did not interact with the important residues (Ser152, His263, Phe77), having structural frame types such as (Table 3)

Table 3. The structural frameworks of group B

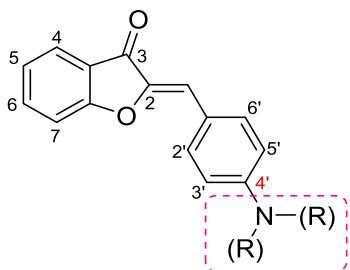
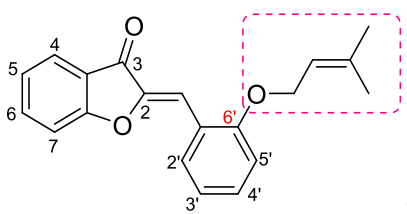
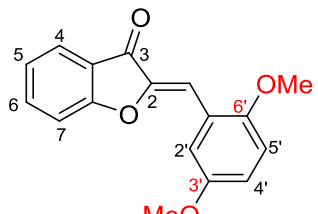
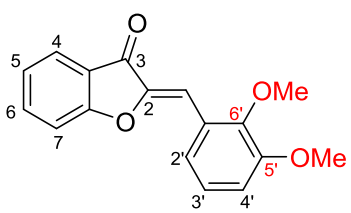
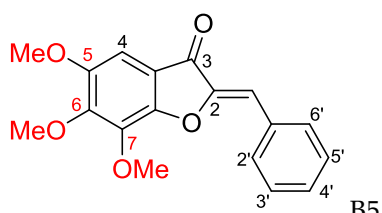
 <p>(R: CH₃, C₂H₅)</p> <p>B1</p> <p>Compounds: A16-17, A27-28, A45, A76</p>	
 <p>B2</p> <p>Compounds: A2, A7</p>	 <p>B3</p> <p>Compounds: A64-65, A67-69, A71</p>
 <p>B4</p> <p>Compounds: A66, A70</p>	 <p>B5</p> <p>Compounds: A22-24, 72</p>

Table 3 showed that the compounds of subgroup B had many adjacent methoxy substituents or the branching substituents, which made the compounds more bulky, difficult to penetrate the catalytic cavity, and did not interact and create bonds with the important residues (Ser152, His163, Phe77).

3.2. A32 compound as the potential compound for the treatment of obesity

In the 82 compounds after carrying out molecular docking, the A32 compound ((Z)-5-chloro-2-(4-(2-(4-methoxyphenyl)-2-oxoethoxy)benzylidene)benzofuran-3(2H)-one) had the best docking result with protein (PDB ID: 1LPB) (docking score: -10.6 kcal.mol⁻¹) and created the bonds with the catalytic triad Ser152-Asp176-His263 and Phe77. According to 5-Lipinski rule, the structure of A32 compound fitted the criteria Table 4), so A32 was suitable for oral drug research.

Table 4. Results of A32 compound assessment according to 5-Lipinski rule

Criteria	5-Lipinski rule	A32 compound
H-bond donors	No more 5	0
H-bond acceptors	No more 10	5
MWT	No more 500 Da	420,85 Da
Log P	No more 5	5,15

A complex of protein 1LPB-A32 was selected to run molecular dynamics simulation, which investigated the stability of protein-ligand complex under the influence of the environment.

3.3. Results of molecular dynamics simulation (MDs)

A complex of protein 1LPB-A32 was run molecular dynamics simulation in 10 ns. At the same condition, the protein without ligand A32 (apoprotein) was also conducted MDs to compare with the results of protein-ligand complex. The results were analyzed following the parameters:

3.3.1. Stability of protein during dynamics simulation (RMSD: Root-mean-square deviation)

The protein structure of the complex with the A32 ligand was more stable than apoprotein in 10 ns of MDs. When starting to 7ns, the RMSD value of the protein in the complex ranged from 1.0 Å to 2.5 Å. After 7 ns, the protein in the complex became more stable with the amplitude fluctuated about 1.0 Å (from 1.0 Å to 2.0 Å). (Figure 3)

3.3.2. Fluctuation of residues during MDs (Root-mean-square fluctuation- RMSF)

The amino acids of apoprotein fluctuated more than the residues of proteins in the complex with A32. Amino acids in the binding region, which created interaction with A32 ligand, had relatively stable with the RMSF value less than 2.0 Å. Especially, residues Ser152, His263, and Phe77 all had RMSF less than 1.0 Å (Figure 4)

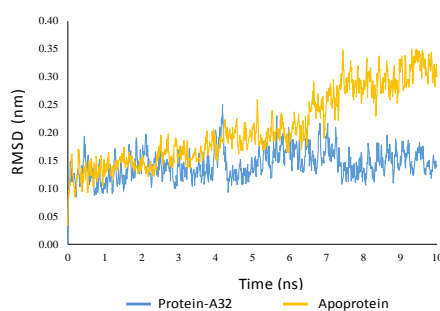


Figure 3. RMSD value of protein backbone (PDB ID: 1LPB) during 10 ns of MDs. Blue is the protein in protein-A32 complex, orange is apoprotein.

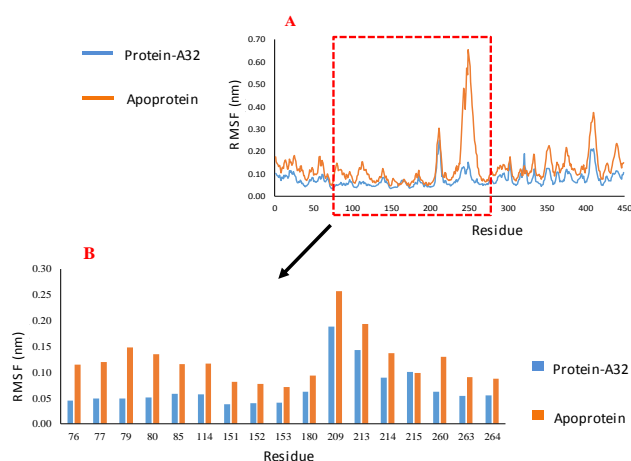


Figure 4. The RMSF value of protein 1LPB during 10 ns of MDs. (A) RMSF value of residues in protein. (B) RMSF value of residues in the binding region. Blue is a protein-A32 complex and orange is apoprotein.

3.3.3. Stability of ligand in MDs (RMSD, RMSF)

After 2 ns, the RMSD value of ligand had an amplitude of oscillation about 0.5 Å (from 0.5 Å to 1.0 Å), showing that the structure of ligand A32 ligand was always stable during 10 ns of MDs. The RMSF value of all atoms in the ligand A32 was less than 1 Å. Especially, O2 and O3 atoms were the main atoms in creating hydrogen bonds with Ser152 and His263, whose RMSF values were respectively 0.4 Å and 0.7 Å. The data demonstrated O2 atoms created bonds with protein more stable than O3 atom (Figure 5)

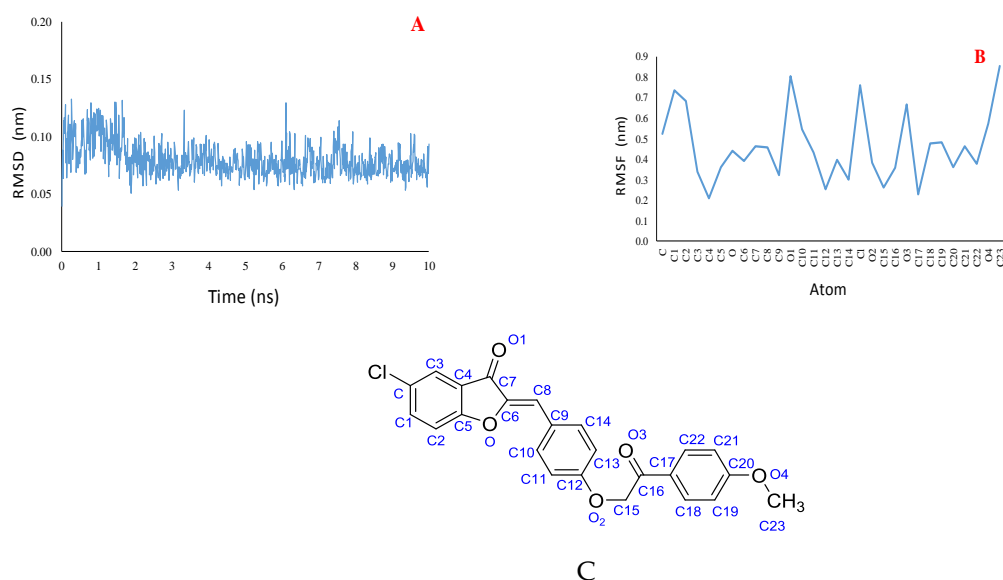


Figure 5. Stability of ligand A32 in complex with protein 1LPB during 10 ns of MDs. (A) RMSD value of ligand A32. (B) RMSF heavy chain atoms of ligand A32. (C) The 2D structure of A32 has atomic numbering.

3.3.4. Occupancies of hydrogen bonds between protein 1LPB and the A32 ligand

The occupancies of hydrogen bonds between the A32 ligand and protein 1LPB, which were determined by VMD software ($d \leq 3.5 \text{ \AA}$ and $\alpha \leq 120^\circ$ [26]). The hydrogen bonds with residues His263 and Phe77 had high expression occupancy, respectively 98.60% and 88.72%. Especially, the occupancy of hydrogen bonding with Ser152 was up to 100.00%. The data proved that the A32 ligand bound well and stable in the catalytic cavity of the HPL during 10 ns of MDs and always interacted with Ser152. The results showed that the compound A32 had potential inhibiting HPL.

3.3.5. Radius of gyration (Rg)

During 10 ns of the process dynamics simulation, the Rg value of the protein in the complex with A32 and apoprotein were average about 2.6 nm, which presented that the protein retained a stable structure during MDs (Figure 6).

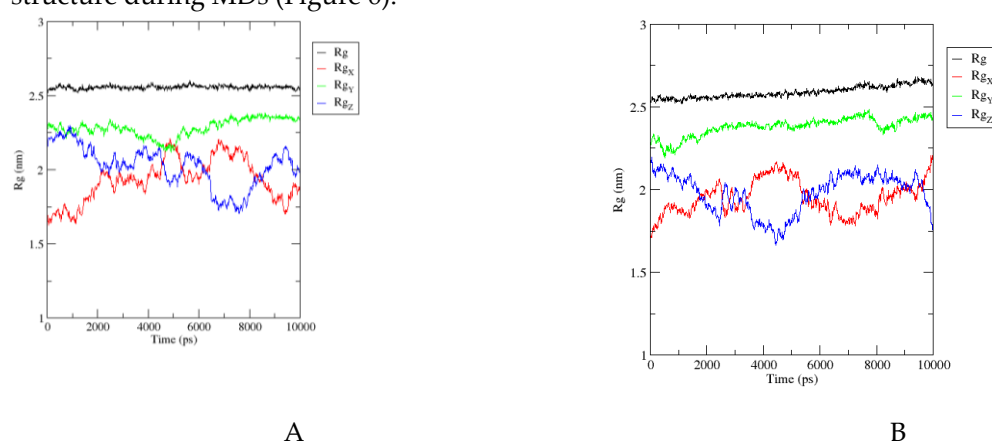


Figure 6. The radius of gyration (Rg) of protein 1LPB during 10 ns of MDs. (A) Rg of protein in complex with ligand A32 (protein-A32). (B) Rg of protein without ligands (apo-protein). Rg (black) is the total radius of gyrate of the protein in space, Rgx (red), Rgy (green), Rgz (blue) are the radius of gyrate of the protein around the x, y, z-axis in space.

3.3.6. Solvent-accessible surface area (SASA)

Figure 7 showed that after 1 ns, SASA of the protein in the complex and apoprotein were reached the maximum value, which had the average value respectively 195 nm² and 200 nm². Once again the results confirmed that binding with A32 ligand contributed to the structural stability of the protein 1LPB (Figure 7).

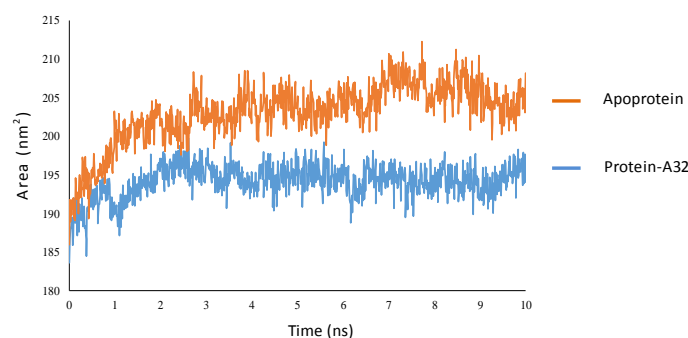
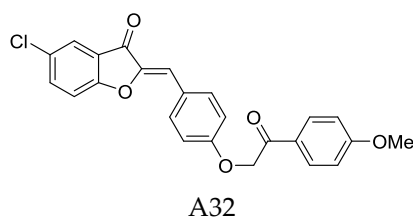


Figure 7. The total solvent-accessible surface area (SASA) of the protein 1LPB is a complex form (protein-A32 - blue) and a non-ligand form (apoprotein - orange).

4. Conclusion



IUPAC name: (Z)-5-chloro-2-(4-(2-(4-methoxyphenyl)-2-oxoethoxy)benzylidene)benzofuran-3(2H)-one

Figure 8. The 2D structure of A32 compound.

Compound A32 (Figure 8) (docking score: 10.6 kcal.mol⁻¹) had the best docking result among 82 aurone derivatives. A32 interacted with the catalytic cavity by hydrogen bonds with Ser152, His151, His263; hydrophobic interaction with Pro180, Phe215, Leu264. A complex of the best binding configuration of A32 with protein 1LPB was run MDs in 10 ns. Combining the molecular docking and MDs, the results showed that A32 compound fitted well into the catalytic cavity of protein 1LPB and maintained the interactions with the catalytic cavity by hydrogen and hydrophobic bonds. Especially, the hydrogen bond with Ser152 was stabilized during the 10 ns MDs, indicating that A32 was a potential compound for resistance to HPL. Therefore A32 compounds could be synthesized and tested *in vitro* as new inhibitors for the anti-HPL effect.

Author Contributions: The authors have done successfully the work such as Han Ai Huynh for investigation and carrying out the research such as molecular docking and molecular dynamics simulations. Phuong Thuy Viet Nguyen for methodology, and validation the results, Dat Van Truong, Van Thi Cam Vo and Dao Thanh Tran for results analysis, Han Ai Huynh writing—original draft preparation, Dao Thanh Tran and Phuong Thuy Viet Nguyen for proof reading and editing the manuscript.

Funding: This research was funded by the NAFOSTED, Viet Nam with the research title “Sàng lọc một số dẫn chất flavonoid tổng hợp có tiềm năng ức chế lipase tụy hướng phát triển thuốc điều trị béo phì”.

Acknowledgments: The authors would like to thank the NAFOSTED for funding to carry out the research entitled “Sàng lọc một số dẫn chất flavonoid tổng hợp có tiềm năng ức chế lipase tụy hướng phát triển thuốc điều trị béo phì”.

Conflicts of Interest: “The authors declare no conflict of interest.”

References

- Schrauwen, P.; Westerterp, K. R. The role of high-fat diets and physical activity in the regulation of body weight. *British Journal of Nutrition* 2000, 84 (4), 417–427.
- Birari, R. B.; Bhutani, K. K. Pancreatic lipase inhibitors from natural sources: unexplored potential. *Drug Discovery Today* 2007, 12(19–20), 879–889
- Lowe Mark, E. Structure and function of pancreatic lipase and colipase. *Annual Review of Nutrition* 1997, 17(1), 141–158.
- Lunagariya, N. A.; Patel, N. K.; Jagtap, S. C.; Bhutani, K. K. Inhibitors of pancreatic lipase: state of the art and clinical perspectives. *EXCLI Journal* 2014, 13, 897–921.
- Won, S.R.; Kim, S.K.; et al. Licochalcone A: A lipase inhibitor from the roots of *Glycyrrhiza uralensis*. *Food Research International* 2007, 40(8), 1046–1050.
- Kumar, S.; Alagawadi, K. R.; Anti-obesity effects of galangin, a pancreatic lipase inhibitor in cafeteria diet fed female rats. *Pharmaceutical Biology* 2013, 51(5), 607–613.

7. Kawaguchi, K.; Mizuno, T.; Aida, K.; Uchino, K.; Hesperidin as an Inhibitor of Lipases from Porcine Pancreas and Pseudomonas. *Bioscience Biotechnology and Biochemistry* 1997, 61(1), 102–104.
8. Zwergel, C.; Gaascht, F.; et al. Aurones: Interesting Natural and Synthetic Compounds with Emerging Biological Potential. *Natural Product Communications* 2012, 7(3), 389–394.
9. Ramawat; Kishan gopal, Natural products: Phytochemistry, Botany and Metabolism of Alkaloids, Phenolics and Terpenes, Springer, Berlin, 2013, 1887–1890.
10. Hassan, G. S.; Georgey, H. H.; George, R. F.; Mohamed, E. R.; Aurones and furoaurones: Biological activities and synthesis. *Bulletin of Faculty of Pharmacy, Cairo University* 2018, 56, 121–127.
11. Winkler F. K. Structure of human pancreatic lipase. *Nature* 1990, 343, 771–774.
12. Lowe Mark E. The triglyceride lipases of the pancreas. *Journal of Lipid Research* 2002, 43(12), 2007–2016.
13. Van Tilbeurgh, H.; Egloff, M.P.; et al. Interfacial activation of the lipase–procolipase complex by mixed micelles revealed by X-ray crystallography. *Nature* 1993, 362(6423), 814–820.
14. Egloff, M. P.; Marguet, F.; Buono, G.; et al. The 2.46 Å Resolution Structure of the Pancreatic Lipase–Colipase Complex Inhibited by a C11 Alkyl Phosphonate. *Biochemistry* 1995, 34(9), 2751–2762.
15. Espinosa Bustos, C.; Cortés Arriagada, D.; et al. Fluorescence properties of aurone derivatives: an experimental and theoretical study with some preliminary biological applications. *Photochemical and Photobiological Sciences* 2017, 16(8), 1268–1276.
16. Elhadi, A. A.; Osman, H.; Iqbal, M. A.; et al. Synthesis and structural elucidation of two new series of aurone derivatives as potent inhibitors against the proliferation of human cancer cells. *Medicinal Chemistry Research* 2015, 24(9), 3504–3515.
17. Hassan, G. S.; Georgey, H. H.; George, R. F.; Mohammed, E. R. Construction of some cytotoxic agents with aurone and furoaurone scaffolds. *Future Medicinal Chemistry* 2018, 10(1), 27–52.
18. Lawrence, N. J.; Rennison, D.; McGown, A. T.; Hadfield, J. A. The total synthesis of an aurone isolated from *Uvaria hamiltonii*: aurones and flavones as anticancer agents. *Bioorganic & Medicinal Chemistry Letters* 2003, 13(21), 3759–3763.
19. Molitor, C.; Mauracher, S. G.; Pargan, S.; et al. Latent and active aurone synthase from petals of *C. grandiflora*: a polyphenol oxidase with unique characteristics. *Planta* 2015, 242(3), 519–537.
20. Yoshihiro Uesawa; Hiroshi Sakagami; et al. Quantitative structure – cytotoxicity relationship of aurones. *Anticancer research* 2017, 37, 6169–6176.
21. Trott, O.; Olson, A. J. AutoDock Vina: Improving the speed and accuracy of docking with a new scoring function, efficient optimization, and multithreading. *Journal of Computational Chemistry* 2010, 31(2), 455–461.
22. Bachwani Mukesh; et al. Molecular docking: A review. *International Journal of Research in Ayurveda & Pharmacy* 2011, 2(6), 1746–1751.
23. Christopher A. Lipinski; et al. Experimental and computational approaches to estimate solubility and permeability in drug discovery and development settings. *Advanced Drug Delivery reviews* 1996, 46, 3–26.
24. Durrant, J. D.; Mc. Cammon, J. A. Molecular dynamics simulations and drug discovery. *BMC Biology* 2011, 9, 2–3.

25. Humphrey, W.; Dalke, A.; Schulten, K. VMD – Visual Molecular Dynamics. *Journal of Molecular Graphics* 1996, 14 (1), 33-38.
26. Lindahl, E. R. *Molecular Dynamics Simulations, Molecular Modeling of Proteins* 2008, 3-23.



© 2019 by the authors. Submitted for possible open access publication under the terms and conditions of the Creative Commons Attribution (CC BY) license (<http://creativecommons.org/licenses/by/4.0/>).